American Journal of
Biomedical Science & Research

www.biomedgrid.com
ISSN: 2642-1747

Research Article

Characterization of an Oil-in-Water Adjuvant and its Interaction with Antigen Protein in Candidate COVID-19 Vaccine

Hua Lyu[1], Xuan Zhou[1], Ping Hu[1], Yang Wang[1]*, Hongwu Du[2]* and Liangzhi Xie[1]*

[1]*Beijing Engineering Research Center of Protein and Antibody, Sinocelltech Ltd., Beijing 100176, China*

[2]*School of Chemistry and Biological Engineering, University of Science and Technology Beijing, China*

***Corresponding author:** Yang Wang and Liangzhi Xie, Beijing Engineering Research Center of Protein and Antibody, Sinocelltech Ltd., Beijing, China.

Hongwu Du, School of Chemistry and Biological Engineering, University of Science and Technology Beijing, Beijing, China; Daxing Research Institute, University of Science and Technology Beijing, Beijing, China.

To Cite This Article: *Yang Wang, Hongwu Du and Liangzhi Xie. Characterization of an Oil-in-Water Adjuvant and its Interaction with Antigen Protein in Candidate COVID-19 Vaccine. Am J Biomed Sci & Res. 2023 19(1) AJBSR.MS.ID.002559,* DOI: 10.34297/AJBSR.2023.19.002559

Received: June 07, 2023; **Published:** June 12, 2023

Abstract

Adjuvants are an essential component in the development of highly effective vaccines. Oil-in-Water (O/W) adjuvants are a class of emulsion suitable for human use to enhance and/or prolong optimal immune response of vaccines. This study characterizes the physical and chemical properties, evaluates the stability of an in-house made O/W squalene-based adjuvant to deepen the understanding of how they may relate to the function of candidate vaccine; Experimental methods and results were used and reported, covering centrifugal stability constant, Turbiscan (a light signal-based) stability, emulsion droplet merging speed, surface tension and *In situ* liquid-transmission electron microscopy, some of which are reported for the first time for studying this type of adjuvant. Furthermore, the interaction between the emulsion adjuvant and the model protein antigens was explored using the Turbiscan stability analysis, isothermal titration calorimetry, size exclusion high performance liquid chromatography, *In situ* liquid-phase transmission electron microscopy, and methods characterizing high-order structure of the model antigen protein (Fourier transform infrared spectroscopy and fluorescent spectrometry), confirming lack of interaction and alternation of antigen structure; Finally, results of adjuvant stability assessment show that the in-house made O/W adjuvant is remarkably stable, due to the optimized component ratio and production process, and highly suitable for used in COVID-19 vaccine.

Keywords: Adjuvant, O/W, Emulsion, Protein antigen, Vaccine, Interaction with adjuvant

Abbreviations: O/W: Oil-in-water; CTL: Cytotoxic T Cells; IFA: Incomplete Freund's Adjuvant; HLB: Hydrophilic-Lipophilic Balance; APC: Antigen-Presenting Cells; CMC: Critical Micelle Concentration; HAS: Human Serum Albumin; ΔBS: Changes Of The Backscattering Light; LPTEM: Liquid-Phase Transmission Electron Microscope; ITC: Isothermal Titration Calorimetry; FTIR: Fourier Transform Infrared Spectroscopy; Try: Tryptophan; Tyr: Tyrosine; Phe: Phenylalanine; ATR: Attenuation Total Reflection; ΔKe: Ke Changes; DLS: Dynamic Light Scattering; PDI: Polydispersity Index.

Introduction

Adjuvants assist the vaccine antigen response and regulate immune response strength and type. The functions of adjuvants for a vaccine are improving the immunogenicity of antigens and the immune response, stimulating Cytotoxic T Cells (CTL), promoting the induction of mucosal immunity, reducing antigen dose, and on set of immunization, improving the immune response of immunocompromised patients, overcoming antigen competition in combination vaccines [1]. The conventional live attenuated vaccines or inactivated vaccines are generally immunogenic, if they generate copies of antigen proteins in the body, some of the carrier proteins

can be used as the inner adjuvant to enhance the immunogenicity. However, most of the protein subunit vaccine antigens (including recombinant vaccines) are weak antigens, and often not effective when administrated alone. Therefore, the addition of the adjuvant is required to potentiate the immune response [2,3]. Aluminum adjuvant became the first adjuvant used globally and the most widely used vaccine adjuvant until now (the size of their particles is 100~1,000 nm). Aluminum-based adjuvants have numerous advantages: safety, low cost, and desired effects to multiple antigens. However, there are also some limitations: it mainly stimulates Th2 reaction, causing non-neutral antibodies or low affinity antibodies to stimulate the body and strengthen inflammation. It is not easily biodegradable. Most of the recombinant antigens are still weak in immunogenicity after combining with aluminum adjuvant [4-13]. Due to the various shortcomings of aluminum adjuvant, the Incomplete Freund's Adjuvant (IFA) was developed in 1951. IFA comprises of liquid paraffin and wool lipids mixed with vaccine antigen to make Water-in-Oil (W/O) latex. The IFA is much more effective than aluminum adjuvant. However, its disadvantage of this adjuvant is that it contains non-degradable oils, with the propensity to form an antigen library on the injection site, causing serious side effects after injection which makes it unsuitable for human vaccines [14]. Notwithstanding the obvious drawback associated with IFA, the fact that it has improved the immunogenicity of many antigens provided the idea for the development of O/W adjuvant. The successfully developed O/W adjuvant was used as an immune enhancer in the late 1980s [15]. Figure 1 shows the composition, morphology and appearance of the in-house made O/W adjuvants, which contains squalene (oil phase), polysorbate 80 (Tween 80; surfactant), and sorbitan trioleate (Span 85; surfactant). The components and formula used in this adjuvant are safe. Squalene is a biodegradable ingredient often derived from shark liver oil [16,17], the low Hydrophilic-Lipophilic Balance (HLB) value surfactant sorbitan trioleate and high HLB value surfactant polysorbate 80 were used as the combined surfactants [18,19] (Figure 1).

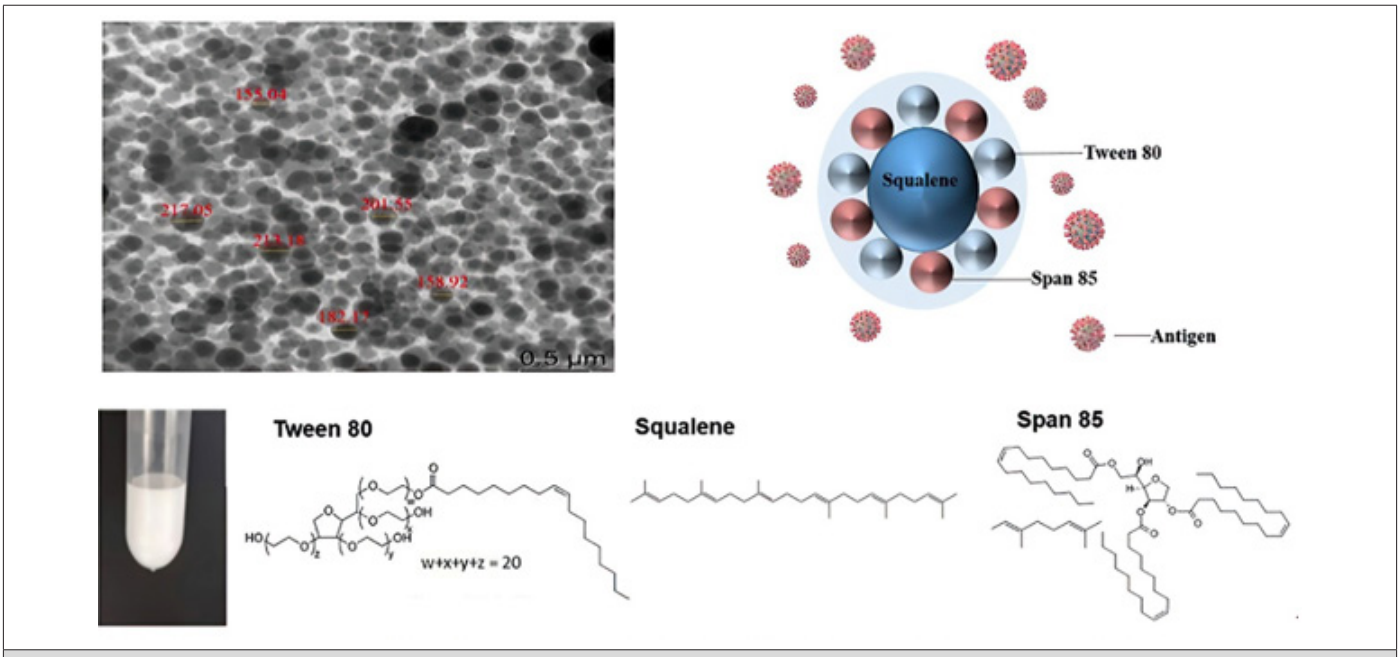

Figure 1: A diagram of the O/W adjuvant.

a) Top left: morphology of the O/W adjuvant under *In situ* liquid-phase transmission electron microscopy (voltage of 300KV).

b) Bottom left: the appearance of the O/W adjuvant (a milky-white emulsion).

c) Top right: schemical composition of the O/W adjuvant (Squalene as the oil phase, Span 85 and Tween 80 as surfactants).

d) Bottom right: molecular formula of the three components of the adjuvant (Squalene, Span 85, Tween 80).

Even though the mechanism of action of adjuvants in vaccine is not entirely clear it primarily falls into three categories. First is its involvement in antigen storage; the antigen changes its physical properties after injecting the antigen and the adjuvant into the body, and this leads to antigen releases slowly [20]. Second is the role it plays in antigen uptake; the adjuvant maintains the antigen conformation and assists with submission to the appropriate immune effect cells, where it induces Th1/Th2 conversion and assists B cell memory and antibody affinity maturation. The final mechanism is targeting function; the adjuvant takes in and transfers antigens through stimulating Antigen-Presenting Cells (APC), then immunization of immune effect cells. Contrastingly, the

main mechanism of action of aluminum adjuvant is antigen storage. While the O/W adjuvant is mainly involved in helping antigen uptake. Notably, there are no interactions between the O/W adjuvant and the antigen before and after intramuscular injection [21]. Meanwhile, the surfactant PS80 in the O/W adjuvant is less likely to interact with protein, because its Critical Micelle Concentration (cmc) is low. *Garidel, et al.* [22] found that polysorbate 20 and PS80 can be combined to the hydrophobic area of Human Serum Albumin (HSA) through hydrogen bonding, to reduce the interaction between the proteins and reduce the accumulation of protein, thus the denaturation temperature of protein increased and the stability enhanced. Therefore, the surfactant polysorbate 80 only interacts with hydrophobic area upon change in the high-order structure of proteins and have no substantial effect on the native structure of proteins, which indicates that polysorbate 80 will not specifically interact with a vaccine antigen. It was reported that the particle size of the O/W adjuvant decreases with increasing concentration of surfactant PS80, and emulsions with smaller particle sizes were more stable [23]. However, there was an article that discussed the possible interaction forces between emulsion type adjuvants and proteins including hydrophobic, electrostatic interactions, but they did not demonstrate the specific experiments [24]. It is unknown and therefore worth exploring whether O/W and recombinant Spike protein interact. Furthermore, according to the WHO requirements, the compatibility and interference between the vaccine and the adjuvant should be appropriately examined [25]. If there is an interaction, advanced technical methods are required to study their impact on conformational structure [26].

Although the use of the Oil in Water (O/W) adjuvant in vaccines has a long history (since 1997), there are fewer research on the physical and chemical properties of this emulsion adjuvant, and little is known about stability properties of the O/W emulsion adjuvant, such as demulsification or aggregation. Therefore, understanding the emulsion integrity of the O/W adjuvant is required in developing an adjuvant for vaccine. Although the emulsion adjuvant enhances the immune response of antigen proteins, it may or may not require interacting with proteins theoretically, presence of interaction between the O/W adjuvant and antigen protein is likely to affect the immunogenicity and safety of vaccine products. Therefore, an investigation of the interaction between the O/W adjuvant and the relative model protein is necessary, which was carried out in this study.

Materials and Methods

Materials

The reagents used in this study include phosphate mobile phase (200mM disodium phosphate, 100 mM arginine, 1% isopropanol, pH 6.50), and they were purchased from sigma chemicals. Squalene, purchased from aasha-biochem; sorbitan trioleate, purchased from Zhaoqing CHAONENG Industry Co., Ltd; polysorbate 80, purchased from Nanjing Well Pharmaceutical Group Co., Ltd. The model proteins used in this work were developed and produced in house, and they are the recombinant SARS-CoV-2 (2019-nCoV) spike protein extracellular domain trimers of the alpha and beta variants. The proteins and their production were published elsewhere [27].

The in-housemade O/W adjuvants were prepared by combining a certain proportion of squalene, sorbitan trioleate and PS80. The oil phase squalene was first added to the water phase, then high shearing force of micro fluidization was used to disperse the emulsion, making the two phases fully mixed to form the milky crude emulsion. Under the actions of the cutting, collision, and acupuncture effect of the microfluidizer's ultra high-pressure homogenizer, the submicron-level emulsion was formed, and the O/W adjuvant was then obtained after sterile filtering.

Experimental Methods

Emulsion Stability Related Properties of the O/W Adjuvant: The emulsion stability related properties of the in-house made O/W adjuvant were systematically studied, sample prepared immediately (T_0 sample), and sample stored at 4°C for 12month (T_{12m} sample) were used to carry out these experiments. The experimental methods include centrifugal stability constant *Ke*, Turbiscan stability, emulsion droplet merging speed K and surface tension.

A Centrifugal Stability Constant *Ke*: For the centrifugal layering analysis, the centrifugal force was used to make different proportions of substances entering into different centrifugal layers. Due to the high-speed rotation of the centrifugal drum, the centrifugal force was far greater than the gravity, and therefore, the centrifugal force made different proportions of substances settled at different speeds. Following a significant particle size change in the O/W adjuvant, the sedimentation speed of large particles and small particles would differ, and the layering occurred. If there was a change in the layering phenomenon in the O/W adjuvant even under low-speed centrifugation, it indicated that the relative stability of this adjuvant was poor. In this the experiment, adjuvant samples were centrifuged at a speed of 1800g to observe whether they were layered. Furthermore, the changes in visible light intensity at wavelength of 500nm before and after the emulsion centrifugation were used to calculate centrifugal stability constant *Ke* (see the following formula). In the formula, A0 and A represent the absorption value at 500 nm before and after centrifuging, respectively. The smaller the *Ke* value, the better the stability. If emulsion droplets merged or demulsified, then *Ke* increased, indicating reductions in stability.

$$Ke = \frac{/A_0 - A/}{A_0} \times 100\%$$

Turbiscan Stability: Turbsican stability analyzer can determine scattering signals of samples without diluting samples, thus achieving the assessment of the stability of emulsions quickly and accurately. The principle which was based on multiple light scattering, two synchronous detectors of transmission light and backscattering light, and a pulsed near infrared light source (λ = 880nm)

was illustrated in Figure 2. The transmission detector was used to study clear and transparent samples, and the backscattering detector was used to study high concentration or particle-containing samples. The O/W adjuvant is a milky-white emulsion with little or no transmitted light. Therefore, the changes of the backscattering light (ΔBS) from the selected backscattering detector were used to characterize the stability of the O/W adjuvant. In this the experiment, we placed adjuvant samples in the detection bottle under the wavelength of 880nm, scanning from the bottom to the liquid surface of the bottle to determine its backscattering light intensity. The following formula was applied to calculate free path of photons and changes of the backscattering light ΔBS, where λ* is the mean free path of photon in the disperse system, φ is the particles volume fraction, d is the particles mean diameter, g and Qs are the optical parameters of Mie theory. The O/W adjuvant consisted of two phases of oil and water, if the emulsions merge, float or sink, that would cause drifting with sinking as well as floating of the Turbiscan diagram baseline (Figure 2).

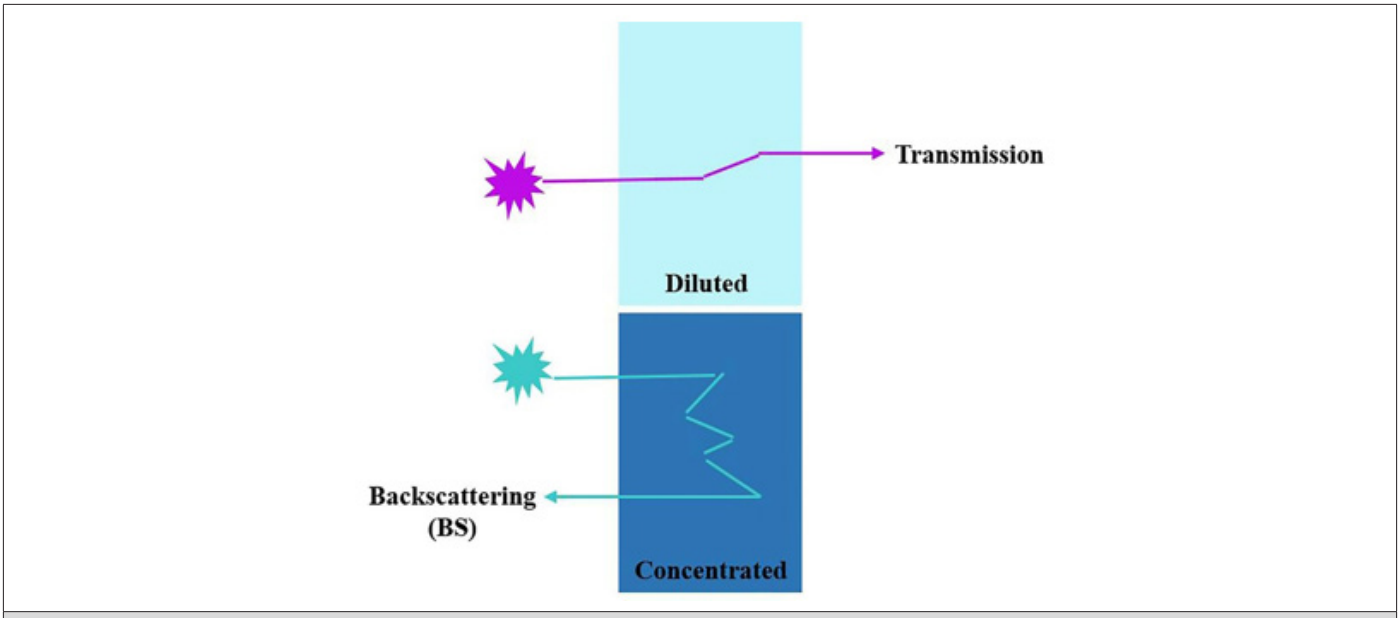

Figure 2: A principle of Turbiscan stability analyzer.

$$BS \approx \frac{1}{\sqrt{\lambda^*}}$$

$$\lambda^*(\varphi, d) = \frac{2d}{3\varphi(1-g)Q_s}$$

a) Transmission means transmission detector, which is used for the analysis clear and transparent samples (diluted).

b) Backscattering (BS) means backscattering detector, which is used for higher concentration or particle-containing samples (concentrated).

c) For the O/W adjuvant in this work, BS is the parameter that can be measured; this figure is derived from an open access publication [28].

Emulsion Droplet Merging Speed *K*: Whether emulsion droplets merged or not is an important stability related property of O/W emulsions. The merging speed constant *K* is calculated by observing the sample under an appropriate microscope and counting the droplets particle number changes within a certain time (such as 60s). The *K* value reflects the trend of emulsion droplets gathering and merging. However, the average particle size of the in-house made O/W adjuvants are around 160nm, which are smaller than the resolution of most optical microscopes, and the O/W structure of the emulsion adjuvants might be destroyed under the vacuum environment of the electron microscope. Therefore, an appropriate microscope that can observe the sub-micron granules is required. A modified Zeiss microscopy was used as its high resolution, fast digital imaging, stable color temperature to observe the sub-micron granules. As the emulsion droplet merging speed follows Newton's first law, the constant *K* can be calculated using the following formula [29], where N is the number of emulsion droplets at time t, N0 is the number of emulsion droplets at time t_0, t is the time, *K* is the merging speed constant. The smaller the *K* value, the more stable the emulsion is. If the O/W adjuvants were merged or broken, the constant *K* would be high. In this experiment, different magnification lenses (20X, 50X) were used, any three fields of view under the microscope were selected and the number of particles was counted using the Icalibur Pro software with a 60s (t) interval in each field of view, then *K* value was calculated. Finally, take the average value of *K* under the three fields of view.

$$\log N = \log N_0 - \frac{kt}{2.303}$$

Emulsion Surface Tension: When the large liquid droplets are scattered into small drops in the O/W adjuvant, the surface free en-

ergy is increased, and the droplets have a tendency to spontaneously reduce the surface area. Therefore, it is necessary to overcome the surface free energy increase in order to maintain stability. The O/W adjuvant was prepared by a high shear and microfluidic method, and the addition of emulsifiers reduced the surface tension to avoid the instability of the emulsion after the external energy disappears. In theory, the surface tension of water is 72mN/m, and the surface tension of oil phase (squalene) is 29mN/m. The surface tension of the O/W emulsion adjuvant should be at the range of 29~72mN/m. The lower the surface tension of the emulsion, the better the stability is. Since the ratio of pressure values of the adjuvant and water is equal to the ratio of their surface tensions. We calculated the emulsion surface tension from the formula below, where σemulsion is the surface tension of the emulsion adjuvant, σ_{water} is the surface tension of water, $\Delta P_{emulsion}$ is the pressure of the emulsion adjuvant, and ΔP_{water} is the pressure of water. If there was merging or demulsification in the sample, its surface tension will be high and closer to water (72mN/m). In this experiment, the tension force was obtained using the pull-off method, where we suspended a microscope slide onto one arm of the balance and immersed it into liquid, the liquid in the container gradually decreased until the slide was pulled off and then recorded the tension force on the balance when the slide was pulled off.

$$\sigma_{emulsion} = \Delta P_{emulsion} / \Delta P_{water} \times \sigma_{water}$$

The Interaction Study of the O/W Adjuvants and Protein Antigens: The adjuvant is an O/W emulsion, the model antigen protein is water-soluble protein, and the final vaccine is prepared after mixing. The proportion of each component of the O/W adjuvant (squalene, Span 85, Tween 80) remains unchanged after mixing. To study the interaction between the adjuvant and the vaccine antigen protein, experimental methods from different aspects were used, including the Turbiscan stability study and SEC-HPLC study that characterize the particle size changes with different principles; the *In situ* LPTEM study characterizes morphology; FTIR and fluorescent spectrometry that characterize the high-order structure of the model proteins.

Turbsican Stability Study: The adjuvant samples in bottle were scanned from the bottom to the liquid surface for about two hours under the wavelength of 880nm, and BS intensity was then determined. When the concentration of the sample was unchanged, BS changes (ΔBS) directly reflected the changes in the particles of the sample over time. The smaller the changes (ΔBS), the more stable the emulsification system. In this experiment, different concentrations (0.05, 0.10 and 0.20mg/mL) of the model proteins and the O/W adjuvant were mixed well, then 3.5mL of mixed samples were placed within the device, scanned from the bottom to the liquid surface. If the model protein interacted with the adjuvant to generate larger particles, particles with different sizes will sink or float differently. Therefore, Turbsican stability analysis can characterize the interaction through molecular size changes.

***In Situ* Liquid-Phase Transmission Electron Microscope (LPTEM) Study:** It is well known that the characterization of biological samples in aqueous media is challenging, as the liquid samples are in continuous flow and cannot stay in a static manner. The *In situ* LPTEM is a powerful technique for directly characterizing samples in the liquid state, it can image samples in their native state, thus achieving the coexistence of the liquid state of sample and the high vacuum environment of the electron microscope. The principle is based on a closed "liquid cell" cavity (contains two oppositely facing Si_3N_4 chips), which limits the liquid sample in a thin layer of less than a few microns Figure 3, and it allows the limited liquid flow inside without being affected by the high vacuum environment outside. Therefore, the morphological structure of the liquid sample can be observed in their original state. The O/W adjuvant and O/W adjuvant-based vaccine were emulsion liquid samples. However, the particle size of the O/W adjuvant was around 160nm while the model protein in the vaccine was only around 10nm, in the same field of vision under the electron microscope, the model protein cannot be observed directly. Therefore, the morphology changes of the O/W adjuvant were used to determine indirectly whether an interaction-induced change occurred or not. If the O/W adjuvant interacted with the protein in vaccine, the morphological structure and particle size of the emulsion in adjuvant sample and vaccine sample (contains the O/W adjuvant and model protein) will be different. Therefore, the *In situ* LPTEM can characterize the interaction through morphological structure changes. In this experiment, 50μL of adjuvant samples, 50μL of vaccine samples (contains 60μg/ml model protein and the adjuvant) were pipetted into the "liquid cell" cavity, respectively, and were placed one end of the observation chip (with a height of 2μm between panes and a film thickness of 30nm) in contact with the liquid surface. The liquid was siphoned into the liquid chamber and the sealing adhesive (glue sealing) was vacuum dried after vacuum extraction for 10min. Then the well-sealed observation chip on the sample operating rod was placed for the *In situ* LPTEM analysis with voltage of 300kV (Figure 3).

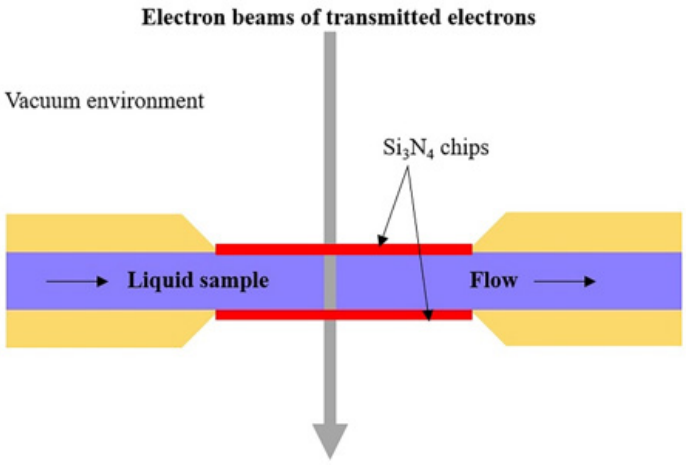

Figure 3: A principle of in situ LPTEM.

Si_3N_4 chips indicate two oppositely facing Si_3N_4 microchips, the liquid sample was sealed in the "liquid cell" cavity and the thickness of the liquid t is small, the electron beam is transmitted through the sample for detection.

Isothermal Titration Calorimetry (ITC) Study: ITC detects the thermodynamic parameters of interaction between the measured molecules. In ITC experiments, the reference cell (contains buffer) and the sample cell (contains the sample) were set to the 25°C; another sample (ligand) was loaded into a syringe which sits in an accurate injection device, and a series of small aliquots of sample (ligand) were injected into the sample cell. The heat sensing devices detected temperature difference between the cells when molecular binding occurred, if there was a binding of the adjuvant to the model protein, heat changes of a few millionths of a degree Celsius were detected and measured. After a number of continuous titrations, the amount of heat released or absorbed between molecules was proportional to the number of molecules. A binding curve was obtained by using the heat generated by the titration (Y-axis) and the molar ratio of titrant and titrated solution (X-axis). Therefore, ITC analysis can characterize the interaction through thermodynamic properties changes. In this experiment, for qualitative analysis, molar concentration of the O/W adjuvant is required. Since the O/W adjuvant was a mixed phase of squalene, polysorbate 80, sorbitan trioleate, etc., its molar concentration was calculated by treating the adjuvant as a sphere of 160nm in diameter, then calculating the number of spheres and further calculating the molar concentration of the adjuvant, which is $7.6*10^{-7}$mol/L. The protein concentration in this experiment is 1.7μM (0.8 mg/mL). ÖThe speed of the stirrer was set at 350 rpm, and the single injection volume of the syringe was 2.02μL, the twice titration interval was 180 s, the syringe volume was 50 μL while the cell volume was 350μL. The Kd value can be calculated to characterize the interaction force (Figure 4).

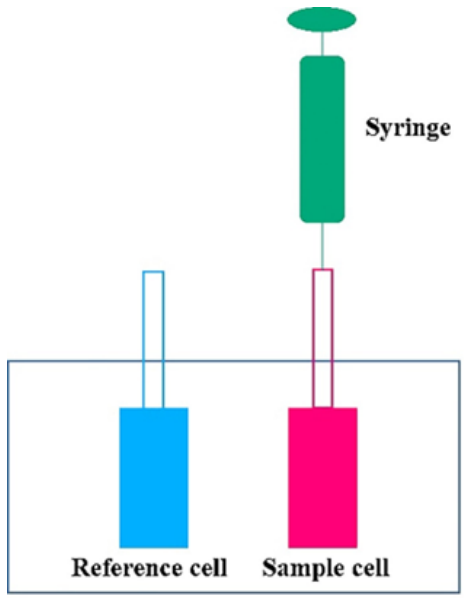

Figure 4: A schematic diagram of ITC principle.

a) Reference cell is used to load a blank control sample (buffer, set at 25°C).

b) Sample cell is used to load the titrated samples (set at 25°C).

c) syringe is used to load titration phase sample.

Size-Exclusion Chromatography (SEC-HPLC) Study: SEC-HPLC is a chromatographic technique that separates molecules within a sample by molecular size. The sample can be separated from large molecules to small molecules. The super large molecules will be excreted from the bed and be the first to be eluted in the dead (or void) volume. Moderate-sized molecules penetrate into the micropores of the chromatographic resin beads (depending on the volume) and elute somewhat slower. The smallest molecules diffuse the deepest in the micropores, which is finally eluted. Therefore, the SEC-HPLC technology can be used to separate molecules with different sizes. If the antigen protein interacted with the O/W adjuvant to form new associated molecular complexes, the retention time of new species was expected to be earlier than the retention time of the protein. Meanwhile, the protein content in free state will be decreased. Therefore, SEC-HPLC technology can characterize the interaction through the free protein content changes. In this experiment, all samples were diluted to protein concentration of 120ug/mL and injected for HPLC analysis. The mobile phase was phosphate mobile phase (200mM disodium hydrogen phosphate, 100mM arginine, 1% isopropanol, pH 6.50), and the elution method was isocratic elution.

Fourier Transform Infrared Spectroscopy (FTIR) Study: The sample molecules absorb infrared light, causing the vibration and rotation of the molecules and their transitioning from lower energy levels to higher energy levels. As a result, selective absorption of specific frequency infrared radiation forms a molecularly and structurally characteristic spectrum, namely infrared spectrum. It is known that this technology can be used to study the secondary structure of protein. If a specific hydrophobic interaction occurred between the antigen protein and the O/W adjuvant, the interaction and environment change were expected to induce protein structural change, and the FTIR spectrum of the protein may be altered. Therefore, FTIR can characterize the interaction through antigen protein secondary structure changes. In this experiment, the model protein sample (3mg/mL), the protein and adjuvant mixed sample (protein: adjuvant=1:1; protein concentration is 3mg/mL) were centrifuged at 12000g for 10min, respectively, and the protein layer was taken for this analysis. The wavenumber range was 1000~2000cm^{-1}, sample and background were scanned 16 times and the resolution of scans was 16cm^{-1}.

Fluorescence Spectroscopy Study: Tryptophan (Try), Tyrosine (Tyr) and Phenylalanine (Phe) in protein molecules can emit fluorescence upon excitation with ultraviolet light. The fluorescent strength of Try is the largest, Tyr is second and the phenylalanine is by far the smallest. The endogenous fluorescence of protein mainly comes from Try and Tyr residues. The fluorescent parameters of Try residues, i.e., the intensity and the peak position, is sensitive to changes of their micro-environment. Try exists in most proteins, and it is often used as an endogenous fluorescent probe to study the consistency of protein high-order structure. If a specific hydrophobic interaction occurred between antigen protein and the O/W adjuvant that alters the micro-environment, the peak of fluorescent spectrum of protein will be blue shifted. Therefore, fluorescent spectrum can characterize interaction through antigen protein high-order structure changes. In this experiment, 1mL of the model protein (3mg/mL), 1mL of the protein and adjuvant mixture sample (protein: adjuvant=1:1, protein concentration is 3mg/mL) were centrifuged at 12000g for 10min, respectively, and the protein layer was taken into the sample chamber for fluorescence spectrophotometer analysis. Experimental parameter settings as 300 scanning times, 32cm^{-1} resolution, automatic atmospheric background deduction and scanning range are 4000-650 cm^{-1}, the sample was evenly spread on the bottom surface of the Attenuation Total Reflection (ATR) prism sample cell, and each sample was scanned 3 times with medium speed.

Instruments : The instruments used in this study include Thermo benchtop microcentrifuge; Klüss KRÜSS K100 surface tensiometer; Zeiss upright microscope AxioLab 5; France FORMULACTION Stability analyzer TURBISCAN Lab; Agilent 1260 HPLC system (Quternary pump G7111A, Autosampler G7129A, Column Oven G7116A, VWD Detector G7114A), SRT-C SEC-500 (4.6×300mm, 5μm) chromatographic column (Sepax Technologies); FEI Tecnai G2 F30 field emission electron microscope, Bio MA-Tek K-kit liquid sample electron microscope *In situ* observation chip (interval height 200nm, film thickness 30nm); Thermo Fisher Fourier Transform Infrared Spectrometer. Agilent Cary Eclipse Fluorescence spectrophotometer. The TA. Instruments Nano Isothermal Titration Calorimeter (ITC).

Results and Discussion

Investigation of Emulsion Stability Related Properties

Result of Centrifugal Stability Constant *Ke*: The three batches of T_0 and T_{12m} samples were centrifuged at a speed of 1,800 g. After the centrifugation, each batch of the adjuvants was not layered. Furthermore, the changes in visible light intensity before and after the centrifuge were detected to calculate *Ke*, according to $Ke=\frac{/A_0-A/}{A_0}\times 100\%$ (where A0 and A represent the absorbance at 500 nm before and after centrifugal). The smaller the *Ke* value, the better the stability. See Table 1 for the experimental results, the *Ke* values at T_0 and T_{12m} were similar (0.34~0.49) with no significant change and no clear trending. There was no literature report on how much *Ke* changes (ΔKe) of nano-emulsions would affect the stability. However, it was reported that the emulsions containing oleic acid or HS15 decreased the centrifugal stability constants, where the constant *Ke* of about 0.5 was considered stable. The emulsions composition in literatures were not completely consistent with the O/W adjuvant emulsion in this work, but the measured centrifugal stability constant *Ke* (0.34~0.49) in this work was similar to the reported constant *Ke* (around 0.5), or even lower than the literature data, indicating the adjuvant emulsions in this work are stable [30] (Table 1).

Table 1: Result of centrifugal stability constant Ke (three batches of the O/W adjuvants at T_0 and T_{12m}).

Sample No	K_e		
	T_0	T_{12m}	ΔK_e
Sample 1	0.34±0.036	0.43±0.004	0.09
Sample 2	0.41±0.012	0.36±0.002	0.05
Sample 3	0.44±0.022	0.49±0.004	0.05

*Note: O/W: Oil-in-water.

Result of Turbiscan Stability: The T_0 and $T_{12\ m}$ samples, and accelerated storage samples (70°C for 1 day and 80°C for 1 day) were placed in the detection bottle, respectively, and the ΔBS was measured. See Figure 5 (left panel) for the spectra, (note that the start of the X-axis represents the bottom of the sample bottle, the end represents the top of the sample bottle, and therefore the measured length of the sample bottle is about 27.5mm). At the top of the bottle, ΔBS peak rises slightly over time, and after shaking the bottle, the curve can return to the baseline, indicating gradual but slight gradient change of two phases (water bulk and larger oil particles). Similar to the settling of aluminum-based adjuvant, this gradient change was not related to the intrinsic stability of the adjuvant. Therefore, the ΔBS rise of the top is because the O/W emulsion form of the adjuvant. A reported soybean protein hydrolysate-stabilized O/W emulsion also showed a similar spectroscopy to our results [31]. As increase of the sample storage temperature, ΔBS tends to the concentration gradient tilt, and the upper floating layer reunites (that is, the formation of large particles), indicating that at 80°C, unstable phenomenon such as layering and gathering will occur.

Furthermore, T_0 sample, T_{12m} sample, and accelerated storage samples (70°C and 80°C for 1 day, respectively) were evaluated by the Dynamic Light Scattering (DLS) detection. See Figure 5 (right panel) for the result, the particle sizes of T_0 and T_{12m} samples were around 160nm, which meets our expectation. The smaller the emulsion sizes, the more stability. After optimizing component ratio and production process, we chose 160nm adjuvant to be used in vaccine. The particle size of the accelerated sample (70°C) remained unchanged (around 160nm), but the PDI increased to >0.1, indicating a trend towards polydisperse particles. The particle size of the accelerated sample (80°C) increased significantly to 176nm, indicating that large particles were generated under this condition. The comparative results between T_0 and T_{12m} will be discussed more in the following Table 3 (Figure 5).

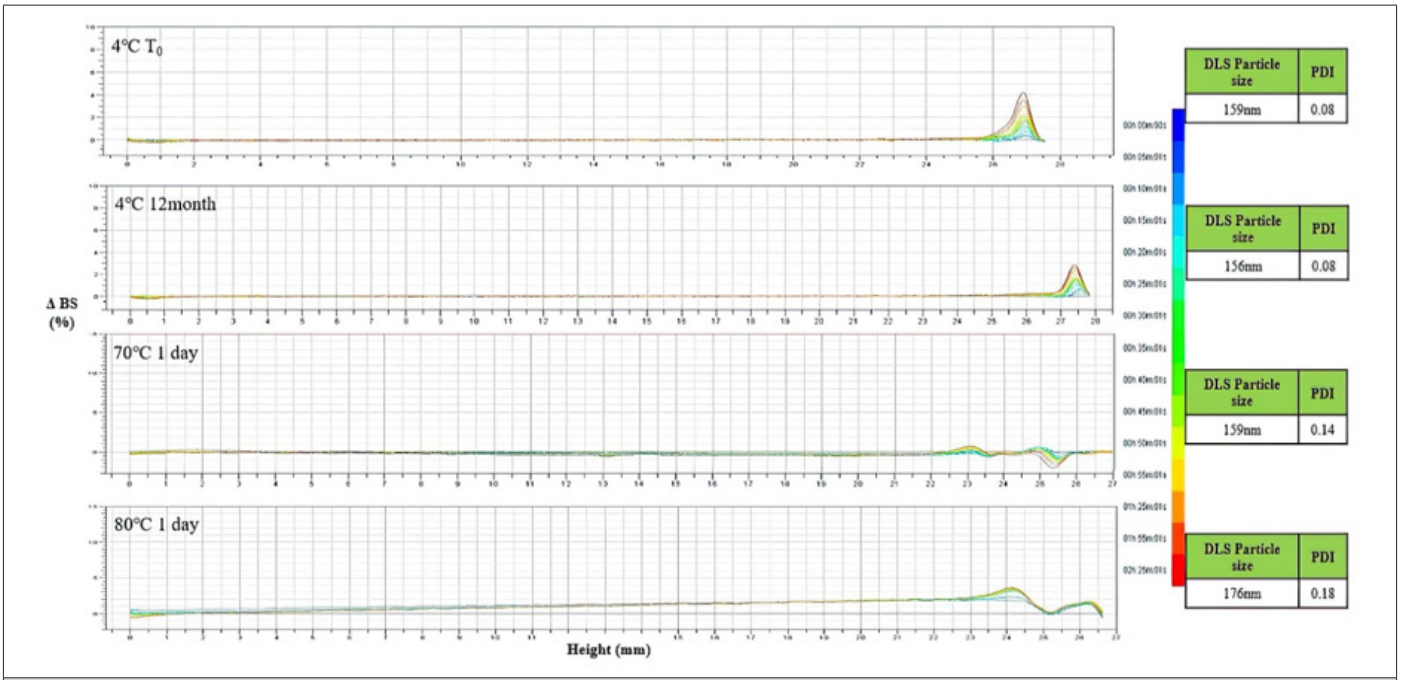

Figure 5: The representative diagram of Turbiscan stability (left panel) and DLS result (right panel).

a) 4°C T_0 means T_0 sample sorted at 4°C, which showed a stable diagram.

b) 4°C 12month means T_{12m} sample sorted at 4°C, which also showed a stable diagram.

c) 70°C 1 day means the accelerated storage samples at 70°C for one day, which showed more peaks at the upper layer.

d) 80°C 1 day means the accelerated storage samples at 80°C for one day, unstable phenomenon occurred.

Result of Emulsion Droplet Merging Speed K: The 3 batches of T_0 and T_{12m} samples were placed on the microscopic slide and monitored under the Zeiss microscope. The number of initial emulsion droplets (N0) and the number of emulsion droplets (N) were observed at T_0 and 60s, respectively, and accounted automatically by the software with the instrument. In the field of view under the Zeiss microscope, the number of emulsion droplets (N0 or N) is generally around 1000. The emulsion droplet merging speed constant K was then calculated according to the formula of . The results are shown in Table 2, the K values of each batch of the O/W adjuvants were small (varies from 1×10^{-4}/s to 6×10^{-4}/s) and consistent after the long-term storage at 4°C ($\Delta K < 6\times10^{-4}$/s). The smaller the K value, the more stable the emulsion. The test results showed that O/W adjuvant was stable during long-term storage at 4°C. Although there was no literature report on emulsion droplet merging speed of this specific O/W adjuvant, it was reported that the coalescence rates between 7.4×10^{-6}/s and 2.5×10^{-4} /s were considered stable for the soybean in water emulsions, where they assumed linear aggregates and considered the coalescence of small flocs [32]. The data in this work is close to that reported data. Another report used molecular dynamics method to investigate the emulsion droplet merging speed of oil in water emulsion and mentioned that the reduction in the surface tension can accelerate the process of droplet merging [33] (Table 2).

Table 2: Result of emulsion droplet merging speed constant K (three batches of the O/W adjuvants at T_0 and T_{12m}).

Batch	*K*		
	T_0 ($\times10^{-4}$/s)	T_{12m} ($\times10^{-4}$/s)	ΔK ($\times10^{-4}$/s)
Sample 1	1±0	6±1	5
Sample 2	4±1	4±1	0
Sample 3	4±1	1±0	3

*Note: O/W: Oil-in-water.

Table 3: Result of DLS detection (three batches of the O/W adjuvants at T_0 and T_{12m}).

DLS	Batch	T_0	T_{12m}
Average Particle Size(nm)	Sample 1	161±1	156±1
	Sample 2	157±2	154±2
	Sample 3	158±1	155±1
Polydispersity Index	Sample 1	0.08±0.02	0.09±0.03
	Sample 2	0.07±0.03	0.08±0.02
	Sample 3	0.05±0.03	0.07±0.03

*Note: O/W: Oil-in-water.

The above results showed that the constant K value is slightly greater than zero, and a small amount of the O/W adjuvant emulsion droplets may have merged. Furthermore, DLS technology was used further for charactering the particle size changes. See Table 3 for the results, the particle size and the Polydispersity Index (PDI) of adjuvants with and without the long-term storage were consistent, the particle sizes were all about 160nm, and PDIs were <0.1. It was reported that nano-emulsion droplets with radii smaller than 2.5μm will mostly behave as non-deformable and stable particles [32]. Thus, under DLS technology, the particle size of the O/W adjuvant was unchanged (around 160nm) after long-term storage at 4°C, no meaningful merging occurred (Table 3).

Result of Emulsion Surface Tension: The 3 batches of T_0 and T_{12m} samples were tested at room temperature and the surface tension calculated following the formula the results were shown in Table 4. After the long-term storage of each batch of adjuvants, the surface tension values varied from 38.5 to 39.5mN/m, which were lower than the surface tension of the water (72mN/m), and higher than the surface tension of the oil phase squalene (29mN/m), and there was no significant difference before and after the long-term storage period. It was reported the higher the surface tension, the higher the surface to kinetic energy ratio of the droplets, and the worse the stability. The emulsion droplets with interfacial tensions of 22.49~42.57 mN/m were considered as stable emulsions [34]. Another paper reported the surface tension of a lignin-based O/W emulsion between 34~39 mN/m, which they considered as a stable emulsified system [35]. Even if the emulsions in literatures are not completely consistent with the O/W adjuvant emulsion in this work, data in literatures can still be used for comparation, and the data in this paper are similar to the literatures, indicating the O/W emulsion is stable (Table 4).

Table 4: Result of emulsion surface tension (three batches of the O/W adjuvants at T_0 and T_{12m}).

Batch	Emulsion Surface Tension (mN/m)		
	T_0	T_{12m}	Δ Surface Tension
Sample 1	38.6	39.5	0.9
Sample 2	38.9	38.9	0
Sample 3	38.5	39.4	0.9

*Note: O/W: Oil-in-water.

Results of the Interaction Between the O/W Adjuvant and Antigen Protein

Turbiscan Stability Study Result: Different concentrations of proteins were mixed with the O/W adjuvant, and then were placed in Turbiscan thermal stabilization instruments. The samples were scanned vertically from bottom to top (the start of X-axis is the bottom of the bottle, the end of X-axis is the top of the bottle, and the scanned length of the sample bottle is about 27.5~28 mm), and ΔBS was recorded repetitively within 2.5 hours. As shown in Figure 6, after mixing O/W adjuvants with 3 different concentrations (0.05mg/mL, 0.1mg/mL, 0.2mg/mL) of the model proteins, no different or abnormal peaks were seen in the diagrams and all of the ΔBS was within 10%, indicating there was no significant interaction between the O/W adjuvant and the model protein. Meanwhile, the diagrams of the 3 samples were consistent, indicating there were no interaction between proteins (low, medium, high concentration) and adjuvant, that is, the protein concentration would not affect the interaction under this technology (Figure 6).

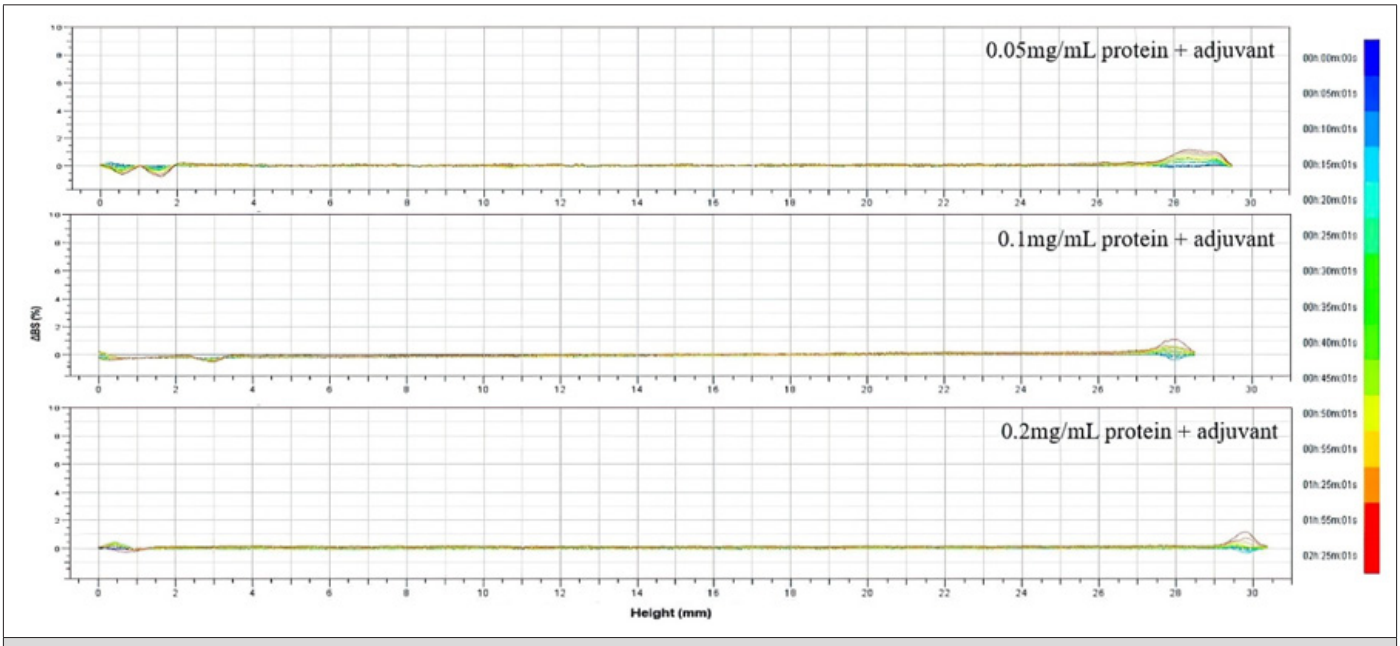

Figure 6: Turbiscan diagram of recombinant protein (with different concentrations) and the O/W adjuvant.

a) 0.05mg/mL model protein mixed with the adjuvant sample (1:1v/v).

b) 0.1mg/mL model protein with the adjuvant sample (1:1v/v).

c) 0.2 mg/mL model protein with the adjuvant sample (1:1v/v).

***In Situ* LPTEM Study Result:** The *In situ* LPTEM was used to observe the morphology of 3 batches of adjuvants and the corresponding 3 batches of drug products. In Figure 7, the 3 images named drug product contained adjuvants and the model antigen proteins, while the 3 images named adjuvant only contained the O/W adjuvant. In all the images, the sample particles distributed evenly (the particle size of the model protein was around 10nm, and therefore, cannot be observed under this microscopy condition). The particle size of samples under this LPTEM was basically the same as the detection results of the DLS analysis, both of which were around 160nm; the emulsion morphology in the O/W adjuvant and the vaccine were consistent with both essentially round shape. Comparing with the reported oleic acid emulsion, both samples showed round shape [36], but O/W adjuvant morphology in this work is denser and more uniform than the reported data (Figure 7).

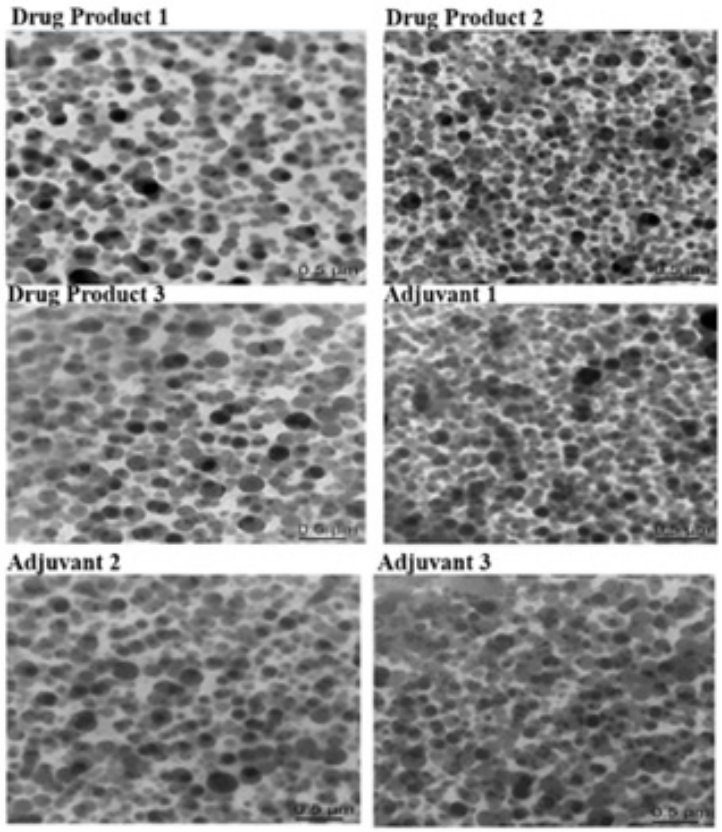

Figure 7: *In-situ* LPEM result of the O/W adjuvant and model vaccine.

a) Drug Product 1, Drug Product 2 and Drug Product 3 mean three batches of the vaccine samples.

b) Adjuvant 1, Adjuvant 2 and Adjuvant 3 mean three batches of the adjuvant samples. All of them were analysed with a voltage of 300kV.

Thus, the emulsion droplets in the O/W adjuvant and the model vaccine were both relatively uniform, distributed evenly and similarly, with no large gathering or merging larger droplets. The morphological structure of the O/W adjuvant has not changed before and after mixing with the model protein at the study concentration, confirming that no effect of interaction can be seen from the perspective of particle morphology.

ITC Study Result: In this study, the model protein was titrated by the adjuvant, and the adjuvant was titrated by the protein, respectively. The concentration of the adjuvant is $7.6*10^{-7}$mol/L, and the protein concentration is 1.7μM (0.8mg/mL). In experiment 1, the adjuvant was the titration phase in 50μL syringe and the model protein in sample cell (350μL) was titrated, and at the end of the titration, the molar ratio between model protein and adjuvant was 15:1. The results of experiment 1 was shown in Figure 8, based on the sequential two site model fitting, the parameters of constant Kd, enthalpy change ΔH, and entropy change ΔS were calculated. The results were shown in Table 5, ΔH>0 indicating that there was a heat absorption response between the adjuvant and the model protein, Kd was 3.372×10^{-7}~1.124×10^{-5} M indicating there was an interaction in the sample cell. Thus, when the ratio between model protein and the adjuvant was 15:1, the interaction was observed under this technology. In experiment 2, the model protein (50μL) titrates the adjuvant (350μL), and at the end of the titration, the molar ratio between model protein and adjuvant was 1:3. The analysis results of Experimental 2 were shown in Figure 9, there are no obvious heat changes in the process of titration, indicating no interaction between model protein and the adjuvant when the ratio between model protein and the adjuvant was 1: 3 (Figure 8).

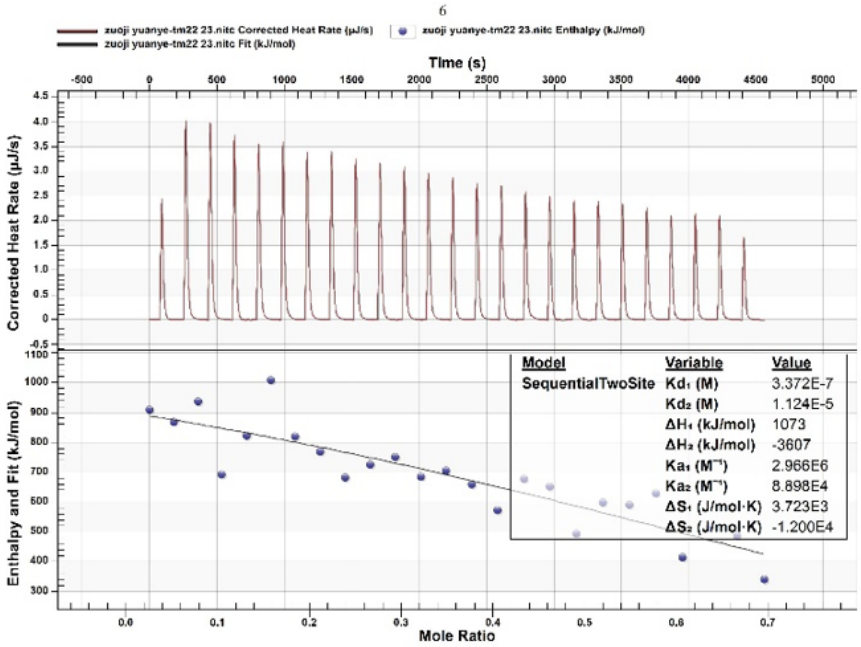

Figure 8: ITC results of Experiment 1: the O/W adjuvant titrates the model protein.

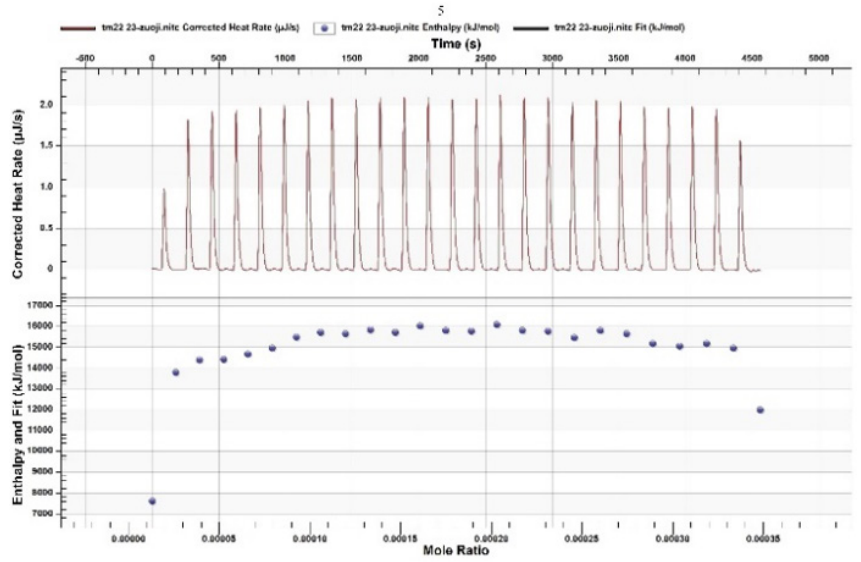

Figure 9: ITC results of Experiment 2: the model protein titrates the O/W adjuvant.

a) For the top graph: Y-axis means the corrected heat rate, X-axis means the titration time.

b) For the bottom graph: Y-axis means the heat generated by the titration, X-axis means the molar ratio of the adjuvant and the model protein (Figure 9).

a) For the top graph: Y-axis means the corrected heat rate, X-axis means the titration time.

b) For the bottom graph: Y-axis means the heat generated by the titration, X-axis means the molar ratio of the model protein and the adjuvant (Table 5).

Generally, under this technology, the concentration ratio of the titration and titrated phase is related to interaction force. When the ratio between model protein and adjuvant was 1:3, there was no interaction. When the ratio between model protein and the adjuvant was 15:1, interaction is occurred. After calculating, the critical affinity force was at the ratio of model protein and the O/W adjuvant was around 2:1.

Table 5: Result of ITC parameters in Experiment 1.

Site	Kd (M^{-1})	ΔH (KJ/mol)	ΔS (KJ/mol)
First	$3.372*10^{-7}$	1073	3723
Second	$1.124*10^{-5}$	-3607	-1200

*Note: O/W: Oil-in-water.

SEC-HPLC Study Result: The following samples were analyzed for SEC-HPLC:

a) 120ug/mL of the monovalent protein (alpha variant, Sample)

b) 120ug/mL of the monovalent protein (beta variant, Sample 2)

c) 120ug/mL of the bivalent model protein (Sample 3, which contained Sample 1: Sample 2 = 1:1, without the O/W adjuvant)

d) vaccine (Sample 4, which contained Sample 3: the adjuvant = 1:1, and protein concentration is 120 ug/mL).

The relative larger adjuvant particles were the first to be eluted in the dead volume and cannot be seen in the chromtogram, only the protein can be seen. Results were shown in Figure 10, most of the model protein in the vaccine (Sample 4) entered the chromatographic column, indicating that the protein in the vaccine was distributed in the water phase of the emulsion. The peak area of all the samples were similar, by examining the differences between the protein recovery rate of Sample 3 (protein) and Sample 4 (protein and adjuvant), whether there were any interactions with the adjuvants can be determined. The quantitative analysis results were shown in Table 6, the results showed that retention time of protein peaks at all samples were the same, indicating the molecule weights of alpha and beta variant protein were similar, under the premise of the testing sample conservation, the peak area of Sample 4 was 92% of Sample 3, that is, the protein content in the vaccine has not changed much compare with protein itself, and the protein can be recovered. Therefore, the model proteins used in this study were not affected by the O/W adjuvant in the vaccine, indicating that the protein did not interact with the adjuvant (Figure 10).

a) S1 means Sample 1.

b) S2 means Sample 2.

c) S3 means Sample 3.

d) S4 means Sample 4 (Table 6).

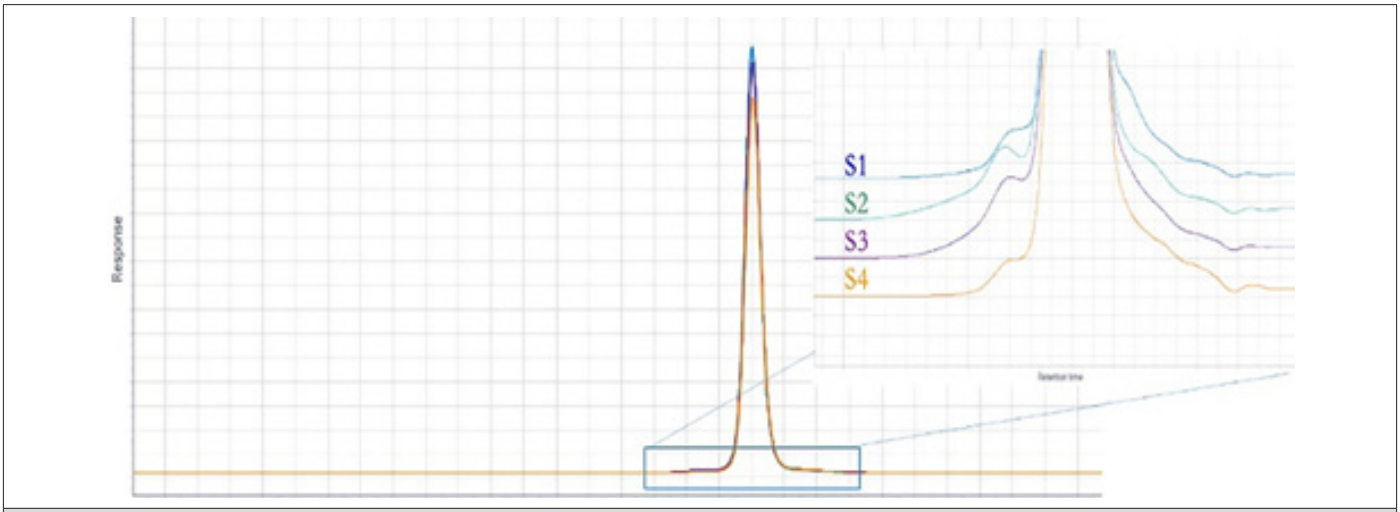

Figure 10: The recovery distribution of model protein in the vaccine by size-exclusion chromatography.

Table 6: SEC-HPLC analysis of the O/W adjuvant and model protein interaction.

No.	Protein Concentration (μg/mL)	Whether Contains adjuvant	Peak Area (LU*s)	The Percentage to Sample 3 Sample
Sample 1	120	No	6345	/
Sample 2	120	No	6226.8	/
Sample 3	120	No	6286.6	100%
Sample 4	120	Yes	5768.6	92%

*Note: O/W: Oil-in-water.

FTIR Study Result: The centrifugation was performed on the adjuvant sample, adjuvant and protein mixed sample. For the sample spectrum results, see Figure 11. For both samples, the peak near 1650cm^{-1} resulted from the C=O stretching vibrations of the peptide bond and the peaks near 1550cm^{-1} resulted from N-H bending vibration or C-N stretching vibration. Furthermore, the results showed that the FTIR spectrum of the model protein was basically the same with or without the adjuvant, confirming that the secondary structure of the protein was not affected by the adjuvant, and there was no specific interaction between the protein and the O/W adjuvant (Figure 11).

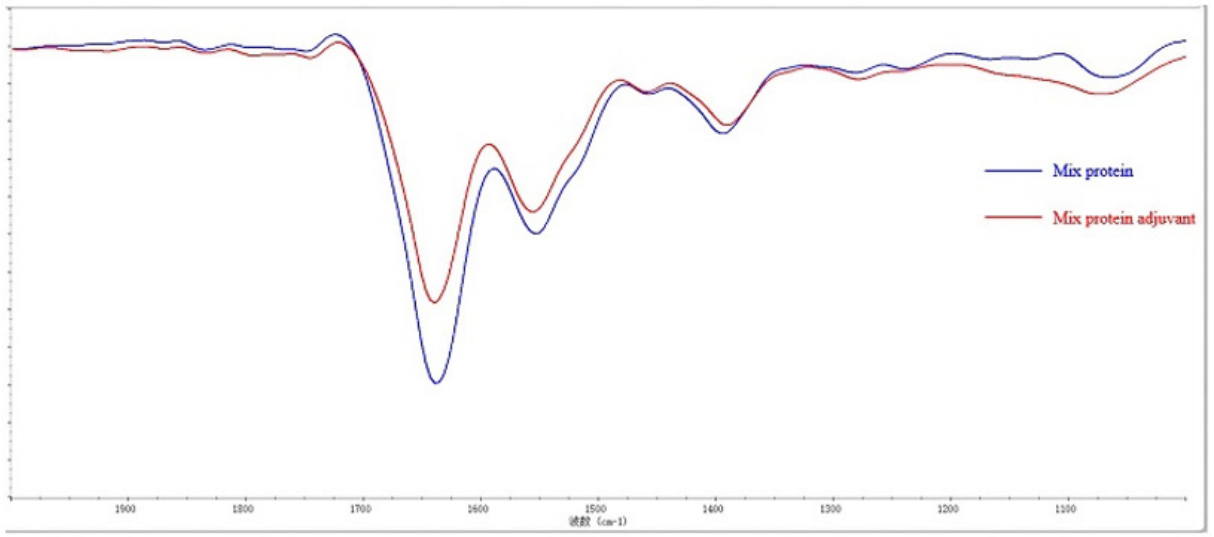

Figure 11: FTIR results of test samples.

a) Mix protein in blue curve mean the model protein.

b) Mix protein adjuvant in red curve means the protein and O/W adjuvant mixed solution.

Fluorescence Spectroscopy Study Result: The model protein sample, the adjuvant and protein mixed sample were performed on fluorescent spectrometry after high-speed centrifugation. See Figure 12 for the results, the curves in the spectrum were basically overlapped and there was no shift of the protein with or without the adjuvant (the maximum wavelength of protein sample was 334nm, while that of adjuvant and protein mixed sample was 336nm), indicating that whether there was the adjuvant or not, the high-order structure of the protein was not changed, and no effect exists on the fluorescence intensity (such as quenching effect), indicating again no specific interaction between the protein and the O/W adjuvant (Figure 12).

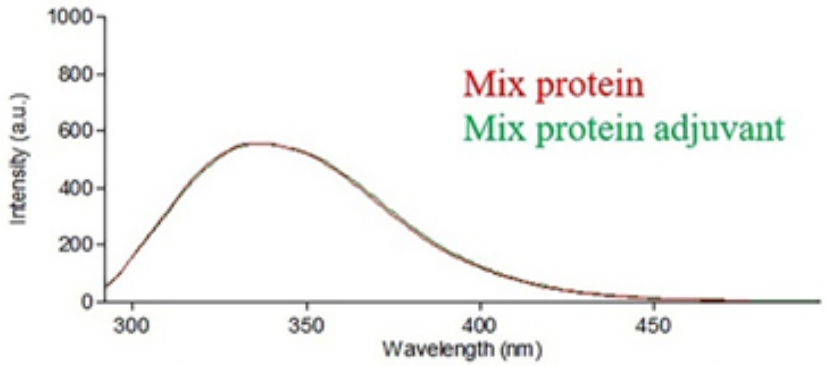

Sample	λmax(nm)
Mix protein	334
Mix protein adjuvant	336

Figure 12: Fluorescent spectrum of the test samples.

a) Mix protein in red curve mean the model protein.

b) Mix protein adjuvant in green curve mean the protein and O/W adjuvant mixed solution.

Conclusion

The widespread use of O/W emulsion adjuvant in vaccines demonstrates its good reliability, safety and tolerability. Even if no serious adverse reactions have been observed in the extensive non-clinical toxicology and safety studies, there is no guarantee that new vaccine or adjuvant formulations would pose no risk to vaccinators, and the unpredictability of adjuvant is related to its own nature, route of administration, antigen dose, antigen nature, and interaction between components. In this work, the emulsion stability related properties of the O/W adjuvant were systematically studied, and the results confirmed that the O/W emulsion with a centrifugal stability constant *Ke* of 0.34~0.49, an emulsion droplet merging speed K of 1×10^{-4}/s to 6×10^{-4} /s, a surface tension of 38.5~39.5mN/m, and a particle size of about 160nm was stable, no droplet merging and demulsification, no droplet breaking even after the 12-month storage at 4°C. The mechanism supporting such good stability steams from the good physical properties of the surfactant containing adjuvant. The surfactants in the O/W adjuvants will properly present at the interface between water and oil phases, reducing its interfacial tension and keeping the emulsion in a relatively stable state. The particle size of the O/W adjuvant decreases with increasing concentration of surfactant PS80, and emulsions with smaller particle sizes and relatively higher concentration of PS80 were more stable. The preparation process of the in-house made O/W adjuvant in this work has been repeatedly optimized, and the O/W adjuvants with particle size of about 160nm were prepared, which were conformed stable by evaluating the emulsion stability properties. Furthermore, the interaction between recombinant COVID-19 antigen proteins and the O/W adjuvant was extensively explored in this work. The experiment results clearly confirmed that there was basically no interaction between the adjuvants and the antigens, resulting in maintaining the intrinsic protein stability. That is, the O/W adjuvant does not affect the structure of the proteins, which might be part of the reason that the related vaccine is highly immunogenic as the way it is structurally designed. As the O/W adjuvants in this work was in-house produced, the stability properties comparison with the literature data is for reference only. Further, we attempted to use extreme environment to demonstrate the stability differences with specific methods. In the Turbiscan diagram, the destroyed adjuvant under 80°C showed fluctuations in sinking and rising, indicating that various properties of the O/W adjuvant are stable under 4°C storage.

In this work, we not only explored specific tests to evaluate the stability of the O/W adjuvant and its interaction with antigen proteins, but also, we provided the results supporting the stability of the O/W adjuvant and its lack of specific interaction with antigen proteins. The work laid groundwork for further characterization of the properties and consistency of this type of adjuvant in vaccine development. In the future, we plan to continue the study of interaction between the O/W adjuvant and other model antigen proteins including a wide range of hydrophobic and hydrophilic types.

Acknowledgements

The authors are also grateful to Dr. Adam Abdul Hakeem Baidoo (from Sinocelltech Ltd.) for the writing and editorial support.

Conflict of Interest

The authors declare that the research was conducted in the absence of any commercial or financial relationships that could be construed as a potential conflict of interest. The intellectual property rights belong to Sinocelltech Ltd., Beijing, China.

References

1. EMEA (2005) Guideline on Adjuvants in Vaccines for Human Use. CHMP pp. 1-18.
2. Li Z, Kang X, Kim KH, Zhao Y, Li Y, et al. (2022). Effective adjuvantation of nanograms of influenza vaccine and induction of cross-protective immunity by physical radiofrequency adjuvant. Sci Rep 12(1): 21249.
3. Araghi A, Taghizadeh M, Hosseini Doost SR, Paradise A, Azimi SM (2022) Evaluation of immunogenicity of Clostridium perfringens type (B) toxoid and inactivated FMD (O) virus with adjuvant (ISA70-MF59). Archives of Razi Institute 78(3): 907-913.
4. Van Cott TC, Jackson HM (2000) Vaccine adjuvants: preparation methods and research protocols edited by Derek O'Hagan, humana press. Trends in Biotechnology 18(12): 511.
5. Su S, Du L, Jiang S (2021) Learning from the past: development of safe and effective COVID-19 vaccines. Nat Rev Microbiol 19(3): 211-219.
6. Munoz FM, Cramer JP, Dekker CL, Dudley MZ, Graham BS, et al. (2021) Vaccine-associated enhanced disease: Case definition and guidelines for data collection, analysis, and presentation of immunization safety data. Vaccine 39(22): 3053-3066.
7. Knudson CJ, Hartwig SM, Meyerholz DK, Varga SM (2015) RSV vaccine-enhanced disease is orchestrated by the combined actions of distinct CD4 T cell subsets. PLoS pathog 11(3): e1004757.
8. Castilow EM, Meyerholz DK, Varga SM (2008) IL-13 is required for eosinophil entry into the lung during respiratory syncytial virus vaccine-enhanced disease. J Immunol 180(4): 2376-2384.
9. Bolles M, Deming D, Long K, Agnihothram S, Whitmore A, et al. (2011) A double-inactivated severe acute respiratory syndrome coronavirus vaccine provides incomplete protection in mice and induces increased eosinophilic proinflammatory pulmonary response upon challenge. J Virol 85(23): 12201-12215.
10. Tseng CT, Sbrana E, Iwata Yoshikawa N, Newman PC, Couch RB, et al. (2012) Immunization with sars coronavirus vaccines leads to pulmonary immunopathology on challenge with the sars virus. PLoS ONE 7(4): e35421.
11. Agrawal AS, Tao X, Algaissi A, Garron T, Narayanan K, et al. (2016) Immunization with inactivated middle east respiratory syndrome coronavirus vaccine leads to lung immunopathology on challenge with live virus. Hum Vaccin Immunother 12(9): 2351-2356.
12. Rothman Alan L (2011) Immunity to dengue virus: a tale of original antigenic sin and tropical cytokine storms. Nat Rev Immunol 11(8): 532-543.
13. Melendi GA, Hoffman SJ, Karron RA, Irusta PM, Laham FR, et al. (2007) C5 modulates airway hyperreactivity and pulmonary eosinophilia during enhanced respiratory syncytial virus disease by decreasing C3a receptor expression. J Virol 81(2): 991-999.

14. Delgado MF, Silvina Coviello, A Clara Monsalvo, Guillermina A Melendi, Johanna Zea Hernandez, et al. (2009) Lack of antibody affinity maturation due to poor Toll-like receptor stimulation leads to enhanced respiratory syncytial virus disease. Nat Med 15(1): 34-41.

15. Gupta RK, Siber GR (1994) Comparison of adjuvant activities of aluminium phosphate, calcium phosphate and stearyl tyrosine for tetanus toxoid. Biologicals 22(1): 53-63.

16. Mendes A, Azevedo Silva J, Fernandes JC (2022) From sharks to yeasts: Squalene in the development of vaccine adjuvants. Pharmaceuticals (Basel)15(3): 265.

17. Fisher KJ, Kinsey R, Mohamath R, Phan T, Liang H, et al. (2023) Semi-synthetic terpenoids with differential adjuvant properties as sustainable replacements for shark squalene in vaccine emulsions. NPJ Vaccines 8(1): 14.

18. Haensler J (2017) Manufacture of oil-in-water emulsion adjuvants. Methods Mol Biol 1494: 165-180.

19. Ott G, Barchfeld GL, Chernoff D, Radhakrishnan R, Hoogevest P, et al. (1995) MF59 design and evaluation of a safe and potent adjuvant for human vaccines. Pharm Biotechnol 6: 277-296.

20. Osebold J W (1982) Mechanisms of action by immunologic adjuvants. J Am Vet Med Assoc 181(10): 983-987.

21. Dupuis M, McDonald D M, Ott G (1999) Distribution of adjuvant MF59 and antigen gD2 after intramuscular injection in mice. Vaccine 18(5-6): 434-439.

22. Garidel P, Hoffmanh C, Blume A (2009) A thermodynamic analysis of the binding interaction between polysorbate 20 and 80 with human serum albumins and immunoglobulins: A contribution to understand colloidal protein stabilization. Biophys Chem 143(1-2): 70-78.

23. Iyer V, Cayatte C, Guzman B, Schneider Ohrum K, Matuszak R, et al. (2015) Impact of formulation and particle size on stability and immunogenicity of oil-in-water emulsion adjuvants. Hum Vaccin Immunother 11(7): 1853-1864.

24. Fox CB, Kramer RM, Barnes VL, Dowling QM, Vedvick TS (2013) Working together: interactions between vaccine antigens and adjuvants. Ther Adv Vaccines 1(1): 7-20.

25. (2014) WHO. Guidelines on the nonclinical evaluation of vaccine adjuvants and adjuvanted vaccines. TRS 987, Annex2: 59-100.

26. Dey AK, Malyala P, Singh M (2014) Physicochemical and functional characterization of vaccine antigens and adjuvants. Expert Rev Vaccines 13(5): 671-685.

27. Sun C, Chi H, Yuan F, Li J, Yang J, et al. (2023) An antibody cocktail with broadened mutational resistance and effective protection against SARS-CoV-2. Sci China Life Sci 66(1): 165-179.

28. Lu Y, Kang W, Jiang J, Chen J, Xu D, et al. (2017) Study on the stabilization mechanism of crude oil emulsion with an amphiphilic polymer using the β-cyclodextrin inclusion method. RSC Adv 7(14): 8156-8166.

29. Guangjin Dong (2010) Preparation and characterizations of 10% fat emulsions for injection [D]. Qingdao University of Science and technolog, master thesis.

30. Xie Y, Chen J, Zhang S, Fan K, Chen G, et al. (2016) The research about microscopic structure of emulsion membrane in O/W emulsion by NMR and its influence to emulsion stability. International Journal of Pharmaceutics 500(1-2): 110-119.

31. Tong X, Cao J, Sun M, Liao P, Dai S, et al. (2021) Physical and oxidative stability of oil-in-water (O/W) emulsions in the presence of protein (peptide): Characteristics analysis and bioinformatics prediction. Lwt, 149: 111782.

32. Rahn Chique K, Puertas AM, Romero Cano MS, Rojas C, Urbina Villalba G (2012) Nanoemulsion stability: experimental evaluation of the flocculation rate from turbidity measurements. Adv Colloid Interface Sci 178: 1-20.

33. Li N, Sun Z, Pang Y, Qi Z, Liu W, et al. (2022) Microscopic mechanism for electrocoalescence of water droplets in water-in-oil emulsions containing surfactant: A molecular dynamics study. Separation and Purification Technology 289: 120756.

34. Antonov DV, Kuznetsov GV, Strizhak PA, Fedorenko RM (2020) Micro-explosion of droplets containing liquids with different viscosity, interfacial and surface tension. Chemical Engineering Research and Design 158: 129-147.

35. Li S, Ogunkoya D, Fang T, Willoughby J, Rojas OJ (2016) Carboxymethylated lignins with low surface tension toward low viscosity and highly stable emulsions of crude bitumen and refined oils. Journal of colloid and interface science 482: 27-38.

36. Wang C, Chen X, Wu Y, Li Y, Cheng S (2020) *In situ* liquid cell transmission electron microscopy observation of dynamic process of oleic acid emulsion with gold nanorods. The Journal of Physical Chemistry C 124(47): 26018-26025.